Journal of Infectious Diseases Advance Access published June 8, 2015

Protective effect of intranasal regimens containing peptidic MERS-CoV fusion inhibitor against MERS-CoV infection

Rudragouda Channappanavar[1,a], Lu Lu[2,a], Shuai Xia[2], Lanying Du[3], David K. Meyerholz[4], Stanley Perlman[1,5], Shibo Jiang[2,3]

[1]Departments of [1]Microbiology, [4]Pathology and [5]Pediatrics, University of Iowa, Iowa City, IA 52242 USA

[2]Key Laboratory of Medical Molecular Virology of Ministries of Education and Health, Shanghai Medical College and Shanghai Public Health Clinical Center, Fudan University, Shanghai 200032, China

[3]Lindsley F. Kimball Research Institute, New York Blood Center, New York, NY 10065, USA

Correspondence: Shibo Jiang, M.D., Key Laboratory of Medical Molecular Virology of Ministries of Education and Health, Shanghai Medical College, Fudan University, 130 Dong An Road, Building #13, Xuhui District, Shanghai 200032, China (shibojiang@fudan.edu.cn) or Stanley Perlman, M.D., Ph.D., Department of Microbiology, University of Iowa, Iowa City, IA 52242, USA (stanley-perlman@uiowa.edu).

[a]RC and LL contributed equally to this work.

Abstract

To gain entry into the target cell, Middle East respiratory syndrome coronavirus (MERS-CoV) utilizes its spike (S) protein S2 subunit to fuse with the plasma or endosomal membrane. We previously identified a peptide derived from the HR2 domain in S2 subunit, HR2P, which potently blocked MERS-CoV S protein-mediated membrane fusion. Here, we tested an HR2P analogue with improved pharmaceutical property, HR2P-M2, for its inhibitory activity against MERS-CoV infection *in vitro* and *in vivo*. HR2P-M2 was highly effective in inhibiting MERS-CoV S protein-mediated cell-cell fusion and infection by pseudoviruses expressing MERS-CoV S protein with or without mutation in the HR1 region. It interacted with the HR1 peptide to form stable α-helical complex and blocked the 6-HB formation between the HR1 and HR2 domains in the viral S protein. Intranasally administered HR2P-M2 effectively protected Ad5-hDPP4-transduced mice from infection by MERS-CoV strains with or without mutations in the HR1 region of S protein, with >1,000-fold reduction of viral titers in lung, and the protection was enhanced by combining HR2P-M2 with interferon β (IFN-β). These results indicate that this combinational regimen merits further development to prevent MERS in high-risk populations, including healthcare workers and patient family members, and to treat MERS-CoV-infected patients.

INTRODUCTION

Severe human respiratory infection caused by the Middle East Respiratory Syndrome (MERS) coronavirus (MERS-CoV) was first identified in 2012 [37]. As of May 25, 2015, 1,139 laboratory-confirmed cases and 431 deaths had been reported to the WHO (http://www.who.int/csr/don/25-may-2015-mers-saudi-arabia/en/). The high case fatality rate among patients with MERS-CoV infection has caused widespread fear because the mode of transmission from zoonotic sources is not well understood, and coronaviruses have the potential to mutate, becoming more pathogenic and transmissible [4,25,29,37]. Bats and dromedary camels are considered to be the natural reservoir and intermediate hosts for MERS-CoV, respectively, but most community-acquired cases are not associated with camel contact [2,17,28,33]. Cumulative evidence from healthcare settings suggest that person-to-person transmission of MERS-CoV can occur through close contact [4,31]. In the absence of an effective vaccine, it is essential to develop strategies to prevent camel-to-human and human-to-human transmission among the high-risk populations, as well as to treat MERS-CoV-infected patients.

MERS-CoV, an enveloped, positive-sense, single-stranded RNA virus, binds to the target cell through interaction between the receptor-binding domain in its spike (S) protein S1 subunit [8,13,24,30,34] and its receptor, dipeptidyl peptidase-4 (DPP4, also known as CD26) [32]. After binding and proteolytic cleavage, a fusion peptide at the N-terminus of S2 is exposed and is inserted into the plasma or endosomal membrane. The heptad repeat 2 (HR2) binds to the heptad repeat 1 (HR1) in S2 to form a six-bundle (6-HB) fusion core, which brings viral and cell membranes into close apposition for fusion [26]. Peptides derived from the HR2 region, such as HR2P, can also interact with HR1 domain in the viral S protein to form heterogeneous 6-HB and

thus block viral fusion with host cell membranes [26], as previously described in the context of HIV and SARS-CoV infections [5,20,22,35].

In the present study, we evaluated an HR2P analogue, designated HR2P-M2, for its *in vitro* and *in vivo* efficacy against infection by the MERS-CoV EMC/2012 strain and strains with mutations in the HR1 domain of the S protein. Most notably, we determined the prophylactic and therapeutic protective activity of HR2P-M2 when used alone or in combination with interferon-β in human DPP4 receptor transduced mice challenged with MERS-CoV.

MATERIALS AND METHODS

Cells and Viruses. 293T cells and Huh-7 cells were obtained from ATCC (Manassas, VA, USA) and the Cell Bank of the Chinese Academy of Science (Shanghai, China), respectively. The EMC/2012 strain of MERS-CoV (passage 8, designated MERS-CoV), provided by Drs. Bart Haagmans and Ron Fouchier (Erasmus Medical Center), was passaged once on Vero 81 cells. Ad5-hDPP4 was developed and propagated by the University of Iowa Gene Transfer Vector Core.

Circular Dichroism (CD) Spectroscopic Analysis

CD spectroscopy was used to determine the secondary structure of the peptides and their complexes [7,23,26,27] as previously described. After CD analysis, thermal denaturation of peptide complexes was immediately monitored using the same sample from 4°C to 100°C at 222 nm with a thermal gradient of 5°C min^{-1}. The [θ]222 value of -33,000 deg cm^2 $dmol^{-1}$ was taken as 100% α-helical content [5,7,26]. Data were further processed using Jasco software.

Native Polyacrylamide Gel Electrophoresis (N-PAGE)

N-PAGE was performed as previously described [22,23]. Peptide HR1P/HR1P-Q1020R/ HR1P-Q1020R (40μM in PBS) was incubated with peptide HR2P-M2 (40μM) at 37ºC for 30 min, respectively, using PBS as control, followed by loading on an 18% Tris-glycine gel with Tricine glycine running buffer (pH 8.3). After staining with Coomassie Blue, images were acquired on a FluorChem Imaging System (Alpha Innotech/ProteinSimple, Santa Clara, CA, USA).

Fluorescence Native Polyacrylamide Gel Electrophoresis (FN-PAGE)

FN-PAGE was carried out in the same manner as N-PAGE described above, except for using FITC-conjugated peptide (HR2P-F). Peptide HR1P/ HR1P-Q1020R/ HR1P-Q1020R (40μM in PBS) was incubated with peptide HR2P-F (40μM) at 37ºC for 30 min, respectively, to form 6-HB, or incubated with increasing concentrations (40, 60 and 80μM) of HR2P-M2 in PBS at 37ºC for 30 min, before addition of HR2P-F, followed by incubation with HR2P-F (40μM) at 37ºC for another 30 min to inhibit 6HB formation. Gels were imaged using a FluorChem 8800 Imaging system with excitation wavelength at 302 nm and emission wavelength at 520 nm. After imaging, the gel was stained with Coomassie Blue and re-imaged.

Inhibition of MERS-CoV S protein-mediated cell-cell fusion

MERS-CoV S protein-mediated cell-cell fusion was tested as previously described [26]. 293T cells transfected with plasmid pAAV-IRES-MERS-EGFP (293T/MERS/EGFP), pAAV-IRES-MERS-Q1020H/EGFP (293T/MERS-Q1020H/EGFP), or pAAV-IRES-MERS-Q1020R/EGFP (293T/MERS-Q1020R/EGFP), respectively, co-expressing the MERS-CoV S protein and EGFP on cell surface, were used as effector cells whereas 293T/EGFP cells,

expressing only EGFP were used as negative control cells. 293T/MERS/EGFP (or 293T/MERS-Q1020H/EGFP, or 293T/MERS-Q1020R/EGFP) and 293T/EGFP cells (1×10^4) were incubated with Huh-7 cells expressing the MERS-CoV receptor DPP4 (5×10^4) as target cells, in the absence or presence of test peptides at the indicated concentrations for 2–4 hrs at 37°C. 293T/MERS/EGFP and 293T/EGFP cells fused, or unfused, with Huh-7 cells were counted under an inverted fluorescence microscope (Nikon Eclipse Ti-S) and the concentration for 50% inhibition (IC_{50}) was calculated using the CalcuSyn software [9].

Inhibition of pseudotyped MERS-CoV infection

Pseudoviruses carrying MERS-CoV S protein with or without mutations were produced as previously described [19,38]. Briefly, pseudovirus was incubated with a test peptide at graded concentration at 37°C for 1 h, followed by addition of the virus/peptide mixture to Huh-7 cells. Cultures were re-fed with fresh medium 12 hrs post-infection and incubated for an additional 48 hrs at 37 °C, followed by addition of luciferase substrate (Promega). Fluorescence was assessed using a luciferase kit (Promega) and an Ultra 384 luminometer (Tecan, San Jose, CA, USA).

Mice

Specific pathogen-free 6- to 12-wk-old C57BL/6 mice and $RAG1^{-/-}$ mice were purchased from the National Cancer Institute and the Jackson Laboratory (Bar Harbor, ME, USA), respectively, and bred at the University of Iowa. All studies were carried out in strict accordance with the recommendations in the Guide for the Care and Use of Laboratory Animals of the National Institutes of Health. Animal experiments were approved by the Institutional Animal Care and Use Committee at the University of Iowa (Protocol #4041009).

Transduction and Infection of Mice

C57BL/6 and RAG1$^{-/-}$ mice were transduced intranasally with 2.5×10^8 PFU of Ad5-hDPP4 in 75μL of DMEM. Five days post-transduction, mice were infected intranasally with wild-type or mutant MERS-CoV (10^5 PFU/50μL of DMEM) and treated intranasally with 50μL of PBS or HR2P-M2 (200μg) peptide alone or in combination with IFN-β. All work with MERS-CoV was conducted in the University of Iowa Biosafety Level 3 (BSL3) Laboratory.

Virus Titers

Lung virus titers were determined using Vero-81 cells as previously described [39]. Virus titers are expressed as PFU/g lung tissue.

Construction of Recombinant Viruses

Recombinant BACs with Q1020R/H mutations were engineered using the Kan^R-I-SceI marker cassette for positive and negative selection as previously described [16]. pBAC-MERS-CoV (a generous gift from Luis Enjuanes) was transformed into GS1783 *E. coli* cells (a generous gift from Greg Smith) containing an arabinose-inducible I-SceI restriction enzyme. A PCR product was generated and transformed into GS1783 cells and recombined with pBAC-MERS-CoV. Recombinant BACs were selected on LB-chloramphenicol-kanamycin plates and verified by restriction enzyme digestion and PCR. The resulting BAC clone was termed pBAC-MERS-CoV Q1020R/H.

RESULTS

HR2P-M2 inhibits MERS-CoV S protein-mediated cell-cell fusion and suppresses infection by pseudoviruses carrying MERS-CoV S protein with mutations in HR1 domain

We tested the inhibitory activity of peptide HR2P-M2, a variant of HR2P (Figure 1*A*), on MERS-CoV S protein-mediated cell-cell fusion using peptides MERS HR2P and SARS CP-1, derived from the HR2 domain of MERS-CoV and SARS-CoV S proteins, respectively [22,26], as controls. Both HR2P-M2 and HR2P strongly inhibited S protein-mediated cell-cell fusion in a dose-dependent manner with IC_{50} values of 0.55 and 0.97 μM, respectively (Figure 1*Ba*), indicating that HR2P-M2 has improved membrane fusion inhibitory activity compared to HR2P. SARS CP-1 peptide did not inhibit MERS-CoV S-mediated cell-cell fusion at concentrations up to 20 μM, confirming our previous observation [26]. The MERS-CoV S protein HR1 domain, the target site of HR2-derived peptides (e.g., HR2P and HR2P-M2), has largely conserved sequences when different strains are compared. Among clinical MERS-CoV strains, only one amino acid change at position 1020 of the HR1 domain (Q1020H or Q1020R) (Figure 1*A*) was observed, and this was present in nearly all strains [1,11]. To test whether HR2P-M2 was effective against these MERS-CoV strains, we compared the inhibitory activity of HR2P-M2 on cell-cell fusion mediated by MERS-CoV S protein, with and without Q1020H or Q1020R mutations. Surprisingly, HR2P-M2 was about 0.9- to 2.6-fold more potent in inhibiting cell-cell fusion mediated by MERS-CoV S protein bearing Q1020H and Q1020R, respectively, than the wild-type S protein of the EMC/2012 strain (Figure 1*Bb*).

Subsequently, we compared HR2P-M2 with HR2P and SARS CP-1 for their inhibitory activity on the entry of pseudovirus expressing MERS-CoV S protein. As shown in Figure 1*Ca*, HR2P-M2 was also more potent than HR2P, with IC_{50} values of 0.61 and 1.21 μM, respectively,

while, again, CP-1 exhibited no inhibition at concentrations up to 20 μM. We then constructed pseudoviruses expressing MERS-CoV S protein with Q1020H or Q1020R mutations and compared their sensitivity to HR2P-M2. Similarly, HR2P-M2 was about 5- to 8-fold more effective in inhibiting infection by the pseudoviruses carrying mutant S protein (Q1020H or Q1020R) than that with the wild-type S protein, while CP-1 displayed no inhibition of either mutant MERS-CoV pseudovirus (Figure 1*Cb-c*). These results suggest that HR2P-M2 is expected to be effective against all MERS-CoV strains isolated so far.

HR2P-M2 interacted with the HR1 peptide to form a stable α-helical complex to block 6-HB formation between the HR1 and HR2 peptides

We previously showed that peptides derived from the MERS-CoV S protein HR1 and HR2 domain (HR1P and HR2P, respectively) could interact together to form stable α-helical complex with α-helicity of ~76% and *T*m value of 87 ^{o}C [26]. Using circular dichroism (CD) spectroscopy, we compared the secondary structures of HR2P-M2, HR1P and its mutants (HR1P-Q1020H and HR1P-Q1020R) and the complexes formed between HR1 and HR2 peptides. As shown in Figure 2*A-C*, HR2P-M2 showed low α-helicity (~6%), while all the HR1 peptides displayed random structures. However, all the complexes formed between HR2P-M2 and the HR1 peptides exhibited α-helical structure with α-helicity in a range of 79% - 88% (Figure 2*A*, 2*B*, and 2*C*), in addition to high *T*m value (91 – 95^{o}C) (Figure 2*D*), suggesting that HR2P-M2 can interact with all these HR1 peptides to form highly stable α-helical complexes.

We then used N-PAGE and FN-PAGE [22,23,26] to further investigate the interaction between HR2P-M2 and HR1P or its mutant. HR1P alone was not detected in the gel (*lanes 1-3*, Figure 3*A*) as this peptide carries a net positive charge and thus migrated out of the gel under native electrophoresis condition [26]. HR2P-M2 alone migrated rapidly (*lane 4*, Figure 3*A*),

while the mixture of HR2P-M2 and HR1P or its mutant migrated more slowly in the gel (*lanes 5-7*, Figure 3*A*). Similarly, HR2P-F alone exhibited a rapidly migrating band (*lane 8*, Figure 3*A*), while the mixture of HR2P-M2 and HR1P or its mutants migrated more slowly in the gel (*lanes 9-11*, Figure 3*A*). These results confirmed that both HR2P-M2 and HR2P-F interact with HR1P and its mutants to form 6-HB.

We subsequently assessed the ability of HR2P-M2 to inhibit 6-HB formation between MERS-CoV HR1 and HR2 peptides using FN-PAGE as previously described [22,23,26]. As shown in Figure 3*B*, the sample containing only HR2P-F (*lane 2*) displayed a single fluorescence band located in the lower portion of the gel, while the mixture of HR1P and HR2P-F (*lane 3*) migrated more slowly. This band corresponded to 6-HB. When increasing concentrations of HR2P-M2 were incubated with HR1P at 37°C for 30 min before addition of HR2P-F (*lanes 4-6*), the fluorescence intensity of the HR2P-F band gradually increased, while that of bands of the complexes corresponding to 6-HB decreased, suggesting that HR2P-M2 inhibited 6-HB formation between the HR1P and HR2P-F in a dose-dependent manner.

HR2P-M2 via intranasal administration inhibited MERS-CoV infection in Ad5-hDPP4-transduced mice

Since mice are impervious to infection with MERS-CoV [10], we sensitized them to infection by transduction with Ad5-hDPP4 [39] prior to testing the *in vivo* efficacy of HR2P-M2 against infection by MERS-CoV EMC/2012, or recombinant MERS-CoV carrying Q1020R or Q1020H mutations in the S protein. HR2P-M2 (200μg) or PBS (control) was intranasally administered to Ad5-hDPP4-transduced mice 6 hrs before challenge with 1×10^5 PFU of MERS-CoV in a total volume of 50μL of DMEM. As shown in Figure 4, viral titers in the lungs of PBS-treated mice challenged with recombinant MERS-CoV carrying WT, Q1020R, or

Q1020H S protein peaked at about 10^6, 10^5, and 10^5, PFU/gm respectively. Strikingly, titers in the lungs of mice treated with HR2P-M2 and challenged with WT, Q1020R, and Q1020H MERS-CoV were decreased to 10^3 PFU/gm (wild type) or below the limit of detection (Q1020R, and Q1020H), representing >1,000-fold reduction of viral titers in lung. The limit of detection (LOD) of the viral titers in our assay was 10^2 PFU/gm, suggesting that mice intranasally treated with HR2P-M2 6 hrs before challenge with MERS-CoV or its variants were highly protected from MERS-CoV infection.

Intranasal application of HR2P-M2 and interferon ß (IFN-β) in combination, before or after viral challenge protected Ad5-hDPP4-transduced mice from MERS-CoV infection

Studies using the HIV-specific peptide enfuvirtide demonstrated the emergence of resistance in the HR1 domain of HIV during prolonged exposure [36]. Therefore, to diminish the likelihood of this occurrence and to provide an additional layer of protection in the event of any emerging resistant virus, we included IFN-β in our prophylactic and therapeutic regimens. IFN-β potently inhibited MERS-CoV infection in cell culture [18], and we previously showed that IFN-β treatment, before or after MERS-CoV challenge, significantly accelerated the kinetics of virus clearance [39].

Initially, we tested the *in vivo* efficacy of IFN-β, HR2P-M2, and their combination as prophylaxis in MERS-CoV-infected C57BL/6 mice. Mice were transduced with Ad5-hDPP4 and treated 5 days later by intranasal administration of PBS, IFN-β, HR2P-M2 or IFN-β/HR2P-M2. Six hrs later, mice were challenged with MERS-CoV, and virus titers were measured at 72 hrs post- infection (p.i.). Virus titers were significantly reduced in all treated groups, with complete clearance observed in mice treated with IFN-β/HR2P-M2 (Figure 5*Aa*). To assess whether these

drugs could be used therapeutically, MERS-CoV-infected Ad5-hDPP4-transduced mice were treated at 12 and 36 hrs p.i., using PBS, IFN-β, HR2P-M2, or IFN-β/HR2P-M2, and virus titers were measured at 96 hrs p.i. As shown in Figure 5*Ab*, titers were significantly decreased in all inhibitor-treated groups ($p<0.003$ compared to PBS-treated group), with the greatest reduction observed in IFN-β/HR2P-M2-treated mice. Additionally, treatment with HR2P-M2 alone resulted in significant reduction in the viral titers in comparison to IFN-β alone treatment groups (Figure 5 A, a-b). Additional cohorts of control mice and mice treated therapeutically were sacrificed at 7 days p.i., and lungs were examined for histological changes. In agreement with our previous report [39], the lungs of MERS-CoV-infected mice showed perivascular, peribronchial and interstitial infiltrates, as well as alveolar septa thickening. However, infiltration was moderately reduced in IFN-β and HR2P-M2 alone treated mice, with pathological changes most attenuated in the IFN-β/HR2P-M2-treated group, consistent with the effects on virus titers (Figure 5*Ab*, *B)*. In no instance was a significant eosinophilic infiltrate detected.

Mice lacking T and B cells (RAG1$^{-/-}$, recombination activation gene 1$^{-/-}$) were unable to clear MERS-CoV with virus detected in the lungs for at least 30 days (data not shown). Therefore, to determine whether IFN-β, HR2P-M2 or IFN-β/HR2P-M2 could enhance virus clearance in the absence of adaptive immune response, MERS-CoV-infected Ad5-hDPP4-transduced RAG1$^{-/-}$ mice were treated prophylactically or therapeutically, as described above for C57BL/6 mice. Prophylactic treatment resulted in enhanced virus clearance at 72 hrs after infection, with complete virus clearance in 1/8 HR2P-M2 and 4/8 IFN-β/HR2P-M2 mice. Similarly, therapeutic treatment at 12 and 36 hrs p.i., with virus titers measured at 96 hrs, revealed significant decreases in virus titers after all therapies ($p<0.005$ compared to PBS-treated). As before, virus titers were reduced to the greatest extent in mice treated with IFN-β/HR2P-M2 (Fig. 5*Ab* and 5*Ad*).

DISCUSSION

Our previous studies demonstrated that peptides derived from MERS-CoV S protein HR2 potently inhibit virus entry, but the present study is the first to show that the peptide functions in the infected lung. From these results, we conclude that peptide is stable in the milieu of the MERS-CoV-infected lung and that intranasal administration delivers peptide to areas of infection with the sufficiency necessary to inhibit virus entry.

So far, no specific antiviral drug has been developed to prevent or treat MERS-CoV infection. Falzarano et al. [15] demonstrated that the combination of ribavirin and IFN-α2b administered to rhesus macaques within 8 hrs of inoculation with MERS-CoV resulted in beneficial effects in reducing virus replication, lung injury and inflammation, thus improving clinical outcome. This ~~treatment~~ combination was also provided to several severely ill patients, and while reducing mortality at 14 days post treatment, it did not show beneficial effects by 28 days, possibly because of late administration [3]. Ribavirin/IFN-a2b in combination with HR2P-M2 together may diminish morbidity and mortality more successfully than either therapy alone. Recently, several compounds from FDA-approved drug libraries were reported to have inhibitory activity against MERS-CoV replication in cell culture [12,14]. We demonstrated that some of these MERS-CoV replication inhibitors could inhibit clathrin-mediated endocytosis, but that most of them did not inhibit MERS-CoV S protein-mediated membrane fusion, and none of them was able to inhibit 6-HB formation [21]. Therefore, these small-molecule MERS-CoV replication inhibitors appear to have mechanisms of action different from that of the peptide MERS-CoV fusion inhibitor HR2P [26].

The HR1 domain in MERS-CoV S protein is the most important target for development of MERS-CoV fusion inhibitors since this region is relatively conserved. Only a single change in the amino acid at position of 1020 in the HR1 domain, namely, Q12020H or Q1020R mutations, has been reported [1,11]. Here we showed that the viruses expressing Q1020H or Q1020R actually grow less well in mouse lung, although they are still potently inhibited by HR2P-M2. Therefore, the peptide targeting the HR1 domain is expected to be effective against most MERS-CoV strains thus far identified.

IFN-β potently inhibited MERS-CoV infection in an *in vitro* cell culture [6,15] and significantly accelerated virus clearance when delivered before or after MERS-CoV challenge, [39]. We now demonstrated that in mice intranasally treated with HR2P-M2 or IFN-β alone or in combination 6 hrs before viral challenge, virus titers in lung were significantly reduced in all treated groups, with complete clearance observed in mice treated with the IFN-β/HR2P-M2 combination (Figure 5*Aa*), verifying their *in vivo* efficacy for prophylactic treatment. We chose to deliver HR2P-M2 and IFN-β intranasally because MERS is predominantly a respiratory tract infection. Since no autopsy or surgical specimens from MERS patients are available, it is not known whether a clinically relevant infection occurs in other organs. Further, MERS-CoV is released from the apical side of respiratory tract cells [40]. Therefore, peptide delivered intranasally would be maximal at the site of infection. Similarly, intranasal administration of the HR2P-M2/IFN-β combination also significantly reduced viral titers in the lungs of RAG1$^{-/-}$ mice, with complete virus clearance in 50% of the treated mice (Figure 5*Ac*), while untreated RAG1$^{-/-}$ mice were unable to clear MERS-CoV for at least 30 days due to a lack of T and B cells [39]. Additionally, intranasal administration of HR2P-M2, IFN-β and their combination to Ad5-hDPP4-transduced C57BL/6 and RAG1$^{-/-}$ mice at 12 and 36 hrs p.i. ~~also~~ resulted in

significant reduction in virus titers in all inhibitor-treated groups, compared to the PBS-treated mice, with virus titers reduced to the greatest extent in mice treated with the IFN-β/HR2P-M2 combination (Figure 5*Ab* and 5*Ad*). Pathological changes in the lungs, such as perivascular, peribronchial and interstitial infiltration, as well as alveolar septa thickening, were moderately reduced in IFN-β and HR2P-M2 alone treated groups with significant attenuation in the IFN-β/HR2P-M2-treated group (Figure 5*B*). Unfortunately, no lung samples from MERS-CoV-infected patients are available; therefore, it is not known whether similar findings would be present in infected humans. However, based on studies of autopsy specimens from patients infected with SARS-CoV, it is likely that severely ill patients would exhibit diffuse alveolar damage. Other than marmosets, no animals experimentally infected with MERS-CoV develop similar disease severity. Once a widely available animal model of severe disease is developed, it will be important to test IFN-β/HR2P-M2 for prophylactic and therapeutic efficacy. It may also be necessary to evaluate different routes of administration of IFN-β and HR2P-M2 if patients or experimentally infected animals are shown to develop significant amounts of systemic disease.

In conclusion, HR2P-M2, a peptide MERS-CoV fusion inhibitor specifically targeting the S protein HR1 domain, is highly effective in inhibiting *in vitro* and *in vivo* infection of divergent MERS-CoV strains. Intranasal application of HR2P-M2, especially in combination with IFN-β, showed high efficacy in accelerating MERS-CoV clearance in animals, suggesting good potential for further development as a prophylactic agent to protect high-risk populations, including healthcare workers and family members of patients infected with MERS-CoV. It also showed efficacy in the treatment of MERS-CoV-infected mice, indicating potential use as a therapeutic agent to treat MERS-CoV-infected patients.

Notes

Financial support. This work was supported by grants from the National Science Fund of China (81173098 and 81361120378 to S.J. and 81373456 to L.L.), the National 973 Program of China (2012CB519001 to S.J.), and grants from the National Institutes of Health (PO1 AI60699 and RO1AI091322 to S.P.). The funder has no role in study designing, data collection, analysis and interpretation, and the manuscript writing.

Potential conflicts of interest. Shibo Jiang and Lu Lu are inventors of the related patent (Chinese patent application No.: 201310099025.7), which has been assigned to Fudan University. Other authors: No reported conflicts of interest.

All authors have submitted the ICMJE Form for Disclosure of Potential Conflicts of Interest. Conflicts that the editors consider relevant to the content of the manuscript have been disclosed.

References

1. List of publicly available sequences and acknowledgements. Website **2014**; http://epidemic.bio.ed.ac.uk/MERS_sequences.

2. Adney DR, van DN, Brown VR, et al. Replication and shedding of MERS-CoV in upper respiratory tract of inoculated dromedary camels. Emerg Infect Dis **2014**; 20:1999-2005.

3. Al-Tawfiq JA, Momattin H, Dib J, Memish ZA. Ribavirin and interferon therapy in patients infected with the Middle East respiratory syndrome coronavirus: an observational study. Int J Infect Dis **2014**; 20:42-6.

4. Assiri A, McGeer A, Perl TM, et al. Hospital outbreak of Middle East respiratory syndrome coronavirus. N Engl J Med **2013**; 369:407-16.

5. Chan DC, Fass D, Berger JM, Kim PS. Core structure of gp41 from the HIV envelope glycoprotein. Cell **1997**; 89:263-73.

6. Chan JF, Chan KH, Kao RY, et al. Broad-spectrum antivirals for the emerging Middle East respiratory syndrome coronavirus. J Infect **2013**; 67:606-16.

7. Chen YH, Yang JT, Chau KH. Determination of the helix and beta form of proteins in aqueous solution by circular dichroism. Biochemistry **1974**; 13:3350-9.

8. Chen Y, Rajashankar KR, Yang Y, et al. Crystal structure of the receptor-binding domain from newly emerged Middle East respiratory syndrome coronavirus. J Virol **2013**; 87:10777-83.

9. Chou TC. Theoretical basis, experimental design, and computerized simulation of synergism and antagonism in drug combination studies. Pharmacol Rev **2006**; 58:621-81.

10. Cockrell AS, Peck KM, Yount BL, et al. Mouse dipeptidyl peptidase 4 is not a functional receptor for Middle East respiratory syndrome coronavirus infection. J Virol **2014**; 88:5195-9.

11. Cotten M, Watson SJ, Zumla AI, et al. Spread, circulation, and evolution of the Middle East respiratory syndrome coronavirus. MBio **2014**; 5:pii: e01062-13.

12. de Wilde AH, Jochmans D, Posthuma CC, et al. Screening of an FDA-approved compound library identifies four small-molecule inhibitors of Middle East respiratory syndrome coronavirus replication in cell culture. Antimicrob Agents Chemother **2014**; 58:4875-84.

13. Du L, Zhao G, Kou Z, et al. Identification of a receptor-binding domain in the S protein of the novel human coronavirus Middle East respiratory syndrome coronavirus as an essential target for vaccine development. J Virol **2013**; 87:9939-42.

14. Dyall J, Coleman CM, Hart BJ, et al. Repurposing of clinically developed drugs for treatment of Middle East respiratory coronavirus infection. Antimicrob Agents Chemother **2014**; 58:4885-93.

15. Falzarano D, de Wit E, Rasmussen AL, et al. Treatment with interferon-[alpha]2b and ribavirin improves outcome in MERS-CoV-infected rhesus macaques. Nat Med **2013**; 19:1313-7.

16. Fehr AR, Perlman S. Coronaviruses: an overview of their replication and pathogenesis. Methods Mol Biol **2015**; 1282:1-23.

17. Gossner C, Danielson N, Gervelmeyer A, et al. Human-Dromedary Camel Interactions and the Risk of Acquiring Zoonotic Middle East Respiratory Syndrome Coronavirus Infection. Zoonoses Public Health **2014**.

18. Hart BJ, Dyall J, Postnikova E, et al. Interferon-beta and mycophenolic acid are potent inhibitors of Middle East respiratory syndrome coronavirus in cell-based assays. J Gen Virol **2014**; 95:571-7.

19. He Y, Lu H, Siddiqui P, Zhou Y, Jiang S. Receptor-binding domain of severe acute respiratory syndrome coronavirus spike protein contains multiple conformation-dependent epitopes that induce highly potent neutralizing antibodies. J Immunol **2005**; 174:4908-15.

20. Jiang S, Lin K, Strick N, Neurath AR. HIV-1 inhibition by a peptide. Nature **1993**; 365:113.

21. Liu Q, Xia S, Sun Z, et al. Testing of middle East respiratory syndrome coronavirus replication inhibitors for the ability to block viral entry. Antimicrob Agents Chemother **2015**; 59:742-4.

22. Liu S, Xiao G, Chen Y, et al. Interaction between heptad repeat 1 and 2 regions in spike protein of SARS-associated coronavirus: implications for virus fusogenic mechanism and identification of fusion inhibitors. Lancet **2004**; 363:938-47.

23. Liu S, Zhao Q, Jiang S. Determination of the HIV-1 gp41 postfusion conformation modeled by synthetic peptides: applicable for identification of the HIV-1 fusion inhibitors. Peptide **2003**; 24:1303-13.

24. Lu G, Hu Y, Wang Q, et al. Molecular basis of binding between novel human coronavirus MERS-CoV and its receptor CD26. Nature **2013**; 500:227-31.

25. Lu L, Liu Q, Du L, Jiang S. Middle East respiratory syndrome coronavirus (MERS-CoV): challenges in identifying its source and controlling its spread. Microbes Infect **2013**; 15:625-9.

26. Lu L, Liu Q, Zhu Y, et al. Structure-based discovery of Middle East respiratory syndrome coronavirus fusion inhibitor. Nat Commun **2014**; 5:3067.

27. Lu M, Blacklow SC, Kim PS. A trimeric structural domain of the HIV-1 transmembrane glycoprotein. Nat Struct Biol **1995**; 2:1075-82.

28. Memish ZA, Mishra N, Olival KJ, et al. Middle East respiratory syndrome coronavirus in bats, Saudi Arabia. Emerg Infect Dis **2013**; 19:1819-23.

29. Memish ZA, Zumla AI, Assiri A. Middle East Respiratory Syndrome Coronavirus Infections in Health Care Workers. N Engl J Med **2013**; 368:2487-94.

30. Mou H, Raj VS, van Kuppeveld FJ, Rottier PJ, Haagmans BL, Bosch BJ. The receptor binding domain of the new MERS coronavirus maps to a 231-residue region in the spike protein that efficiently elicits neutralizing antibodies. J Virol **2013**; 87:9379-83.

31. Perlman S, McCray PB, Jr. Person-to-person spread of the MERS coronavirus--an evolving picture. N Engl J Med **2013**; 369:466-7.

32. Raj VS, Mou H, Smits SL, et al. Dipeptidyl peptidase 4 is a functional receptor for the emerging human coronavirus-EMC. Nature **2013**; 495:251-4.

33. Reuss A, Litterst A, Drosten C, et al. Contact investigation for imported case of Middle East respiratory syndrome, Germany. Emerg Infect Dis **2014**; 20:620-5.

34. Wang N, Shi X, Jiang L, et al. Structure of MERS-CoV spike receptor-binding domain complexed with human receptor DPP4. Cell Res **2013**; 23:986-93.

35. Wild CT, Shugars DC, Greenwell TK, McDanal CB, Matthews TJ. Peptides corresponding to a predictive alpha-helical domain of human immunodeficiency virus type 1 gp41 are potent inhibitors of virus infection. Proc Natl Acad Sci USA **1994**; 91:9770-4.

36. Xu L, Pozniak A, Wildfire A, et al. Emergence and evolution of enfuvirtide resistance following long-term therapy involves heptad repeat 2 mutations within gp41. Antimicrob Agents Chemother **2005**; 49:1113-9.

37. Zaki AM, van Boheemen S, Bestebroer TM, Osterhaus ADME, Fouchier RAM. Isolation of a novel coronavirus from a man with pneumonia in Saudi Arabia. N Engl J Med **2012**; 367:1814-20.

38. Zhao G, Du L, Ma C, et al. A safe and convenient pseudovirus-based inhibition assay to detect neutralizing antibodies and screen for viral entry inhibitors against the novel human coronavirus MERS-CoV. Virol J **2013**; 10:266.

39. Zhao J, Li K, Wohlford-Lenane C, et al. Rapid generation of a mouse model for Middle East respiratory syndrome. Proc Natl Acad Sci U S A **2014**; 111:4970-5.

40. Zielecki F, Weber M, Eickmann M, et al. Human cell tropism and innate immune system interactions of human respiratory coronavirus EMC compared to SARS-coronavirus. J Virol **2013**; 87:5300-4.

FIGURE LEGENDS

Figure 1. Schematic illustration of the MERS-CoV S2 subunit HR1 and HR2 domains and inhibition of MERS-CoV infection. *A,* Sequences of the peptides derived from the HR1 and HR2 domains of MERS-CoV S protein S2 subunit. *B,* Inhibition of cell-cell fusion mediated by MERS-CoV S protein without mutation (*a*) and with Q1020H or Q1020R mutation (*b*). *C,* Inhibition of infection by pseudoviruses expressing S protein of MERS-CoV EMC/2012 strain (*a*), or S protein with Q1020H (*b*) or Q1020R (*c*). Each sample was tested in triplicate, and the experiment was repeated twice. Data from a representative experiment shown (mean ± SD (bar)).

Figure 2. Interaction of HR2P-M2 with HR1P or its mutant to form stable α-helical complexes. Circular dichroism (CD) spectroscopic analysis of the secondary structure of the complex formed by HR2P-M2 peptide and HR1P (*A*), HR1P-Q1020H (*B*), or HR1P-Q1020R (*C*). The circular dichroism spectra for the individual peptides and in complex in phosphate buffer (pH 7.2) at 4°C are shown. (*D*) CD signal at 222 nm for the HR1P/HR2P complex as a function of temperature. The curve of the first derivative (d[θ]/dT) against temperature (T) was used to determine the *Tm* value.

Figure 3. HR2P-M2 inhibition of 6-HB formation between HR1 and HR2 peptides.

A, Determination of 6-HB formation between HR2P-M2, or HR2P-F, and HR1P, or its mutant, by N-PAGE (the upper panel) and FN-PAGE (lower panel). Mixtures of HR1 and HR2 peptides at a final concentration of 40μM were incubated at 25 °C for 30 min before electrophoresis. The fluorescence bands in the gel were first imaged using a FluorChem 8800 Imaging System and a transillumination UV light source. The gel was then stained with Coomassie Blue and imaged again with the FluorChem 8800 Imaging System. *B,* HR1P was incubated with HR2P-M2, followed by the addition of HR2P-F, and inhibitory activity against 6-HB formation was detected

by FN-PAGE. Specifically, HR1P was incubated with increasing concentrations (40, 60, and 80 μM) of HR2P-M2 at 37 ºC for 30 min before addition of HR2P-F. After incubation at 37 ºC for another 30 min, the mixture was loaded to the gel. The fluorescence bands in the gel were first imaged by the FluorChem 8800 Imaging System using a transillumination UV light source.

Figure 4. Inhibition of MERS-CoV infection in Ad5 hDPP4-transduced mice by intranasal administration of HR2P-M2 alone before viral challenge.

Ad5-hDPP4-transduced C57BL/6 mice were treated intranasally with 200μg of HR2P-M2 or PBS only, respectively, as described in the Materials and Methods. Six hrs later, mice were infected with 1×10^5 PFU of WT MERS-CoV, Q1020H-MERS-CoV or Q1020R-MERS-CoV in 50μL of DMEM. Virus titers were determined on day 3 p.i. as described earlier [39]. Data are representative of two independent experiments with 3-4 mice/group/experiment. Statistical significance was determined by an unpaired Student's -*t* test. ****-P<0.0001, PBS compared to HR2P-M2-treated groups in WT MERS-CoV, Q1020H-MERS-CoV or Q1020R-MERS-CoV infected C56BL/6 mice.

Figure 5. Inhibition of MERS-CoV infection in Ad5 hDPP4-transduced mice by intranasal application of HR2P-M2-containing regimens before and/or after viral challenge. *A*, Determination of virus titers in the lungs of MERS-CoV-infected Ad5 hDPP4-transduced C57BL/6 and $RAG1^{-/-}$ mice treated with IFN-β, HR2P-M2, or IFN-β+HR2P-M2. *a* and *c*, Ad5-hDPP4-transduced C57BL/6 (*a*) and $RAG1^{-/-}$ mice (*c*) were intranasally treated with 2000 U of IFN-β, 200μg of HR2P-M2, both IFN-β (2000 U) and HR2P-M2 (200μg), or PBS only,

respectively, as described in the Methods. Six hrs later, mice were infected with 1×10^5 PFU MERS-CoV in a total volume of 50µL of DMEM. Virus titers were determined on day 3 p.i. as described earlier [39]. *b* and *d*, Ad5-hDPP4-transduced C57BL/6 (*b*) and RAG1$^{-/-}$ mice (*d*) were infected intranasally with 1×10^5 PFU MERS-CoV in a total volume of 50µL of DMEM. At 12 hrs and 36 hrs p.i., mice were treated intranasally with 2000 U of IFN-β, 200µg of HR2P-M2 both IFN-β (2000 U) and HR2P-M2 (200µg), or PBS only, respectively. Virus titers were determined on day 4 p.i.. Data are representative of two independent experiments with 4 mice/group/experiment. Statistical significance was determined by an unpaired Student's -*t* test. (a) $^{\Delta}P<0.001$, PBS compared to other groups; $^{*}P<0.02$, IFN-β compared to other treated groups; $^{\#}P<0.01$, HR2P-M2 *vs*. IFN-β + HR2P-M2. (b) $^{\Delta}P<0.01$, PBS compared to other groups; $^{*}P<0.03$, IFN-β compared to other treated groups; $^{\#}P<0.01$, HR2P-M2 *vs*. IFN-β + HR2P-M2. (c) $^{\Delta}P<0.002$, PBS compared to other groups; $^{*}P<0.01$, IFN-β compared to other treated groups. (d) $^{\Delta}P<0.01$, PBS compared to other groups; $^{*,\#}P<0.01$, IFN-β + HR2P-M2 compared to IFN-β or HR2P-M2, respectively. *B*, Histological examination of lungs from MERS-CoV-infected, Ad5-hDPP4-transduced C57BL/6 mice at 7 days p.i. Ad5-hDPP4-transduced C57BL/6 were infected intranasally with 1×10^5 PFU MERS-CoV in a total volume of 50µL of DMEM. At 12 hrs and 36 hrs post-MERS-CoV infection, mice were treated intranasally with 100 µL (50 µL + 50 µL at 10 min intervals) of PBS containing 2000 U of IFN-β, 200µg of HR2P-M2, both IFN-β (2000 U) and HR2P-M2 (200µg) or PBS only, respectively. Lungs were removed at day 7 p.i., fixed in zinc formalin and paraffin embedded. Sections were stained with hematoxylin and eosin (original magnification: 10x).

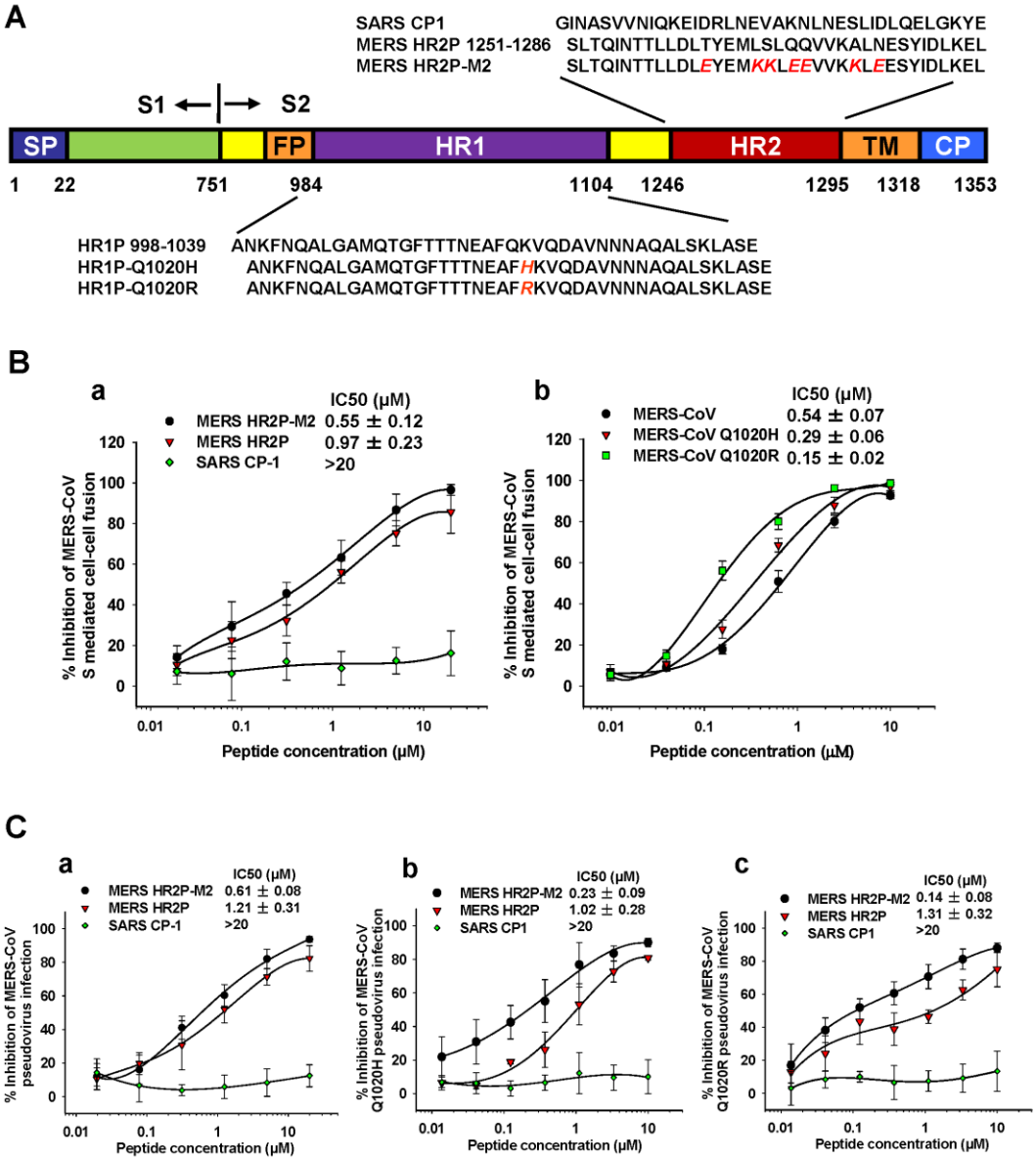

Figure 1

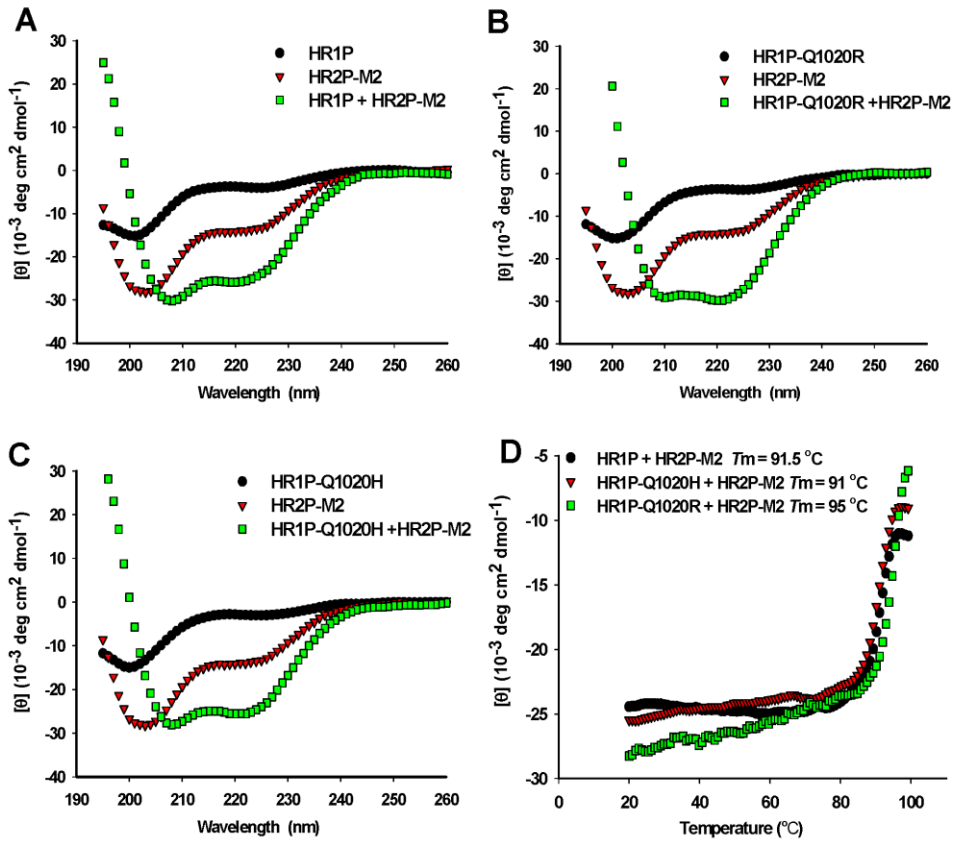

Figure 2

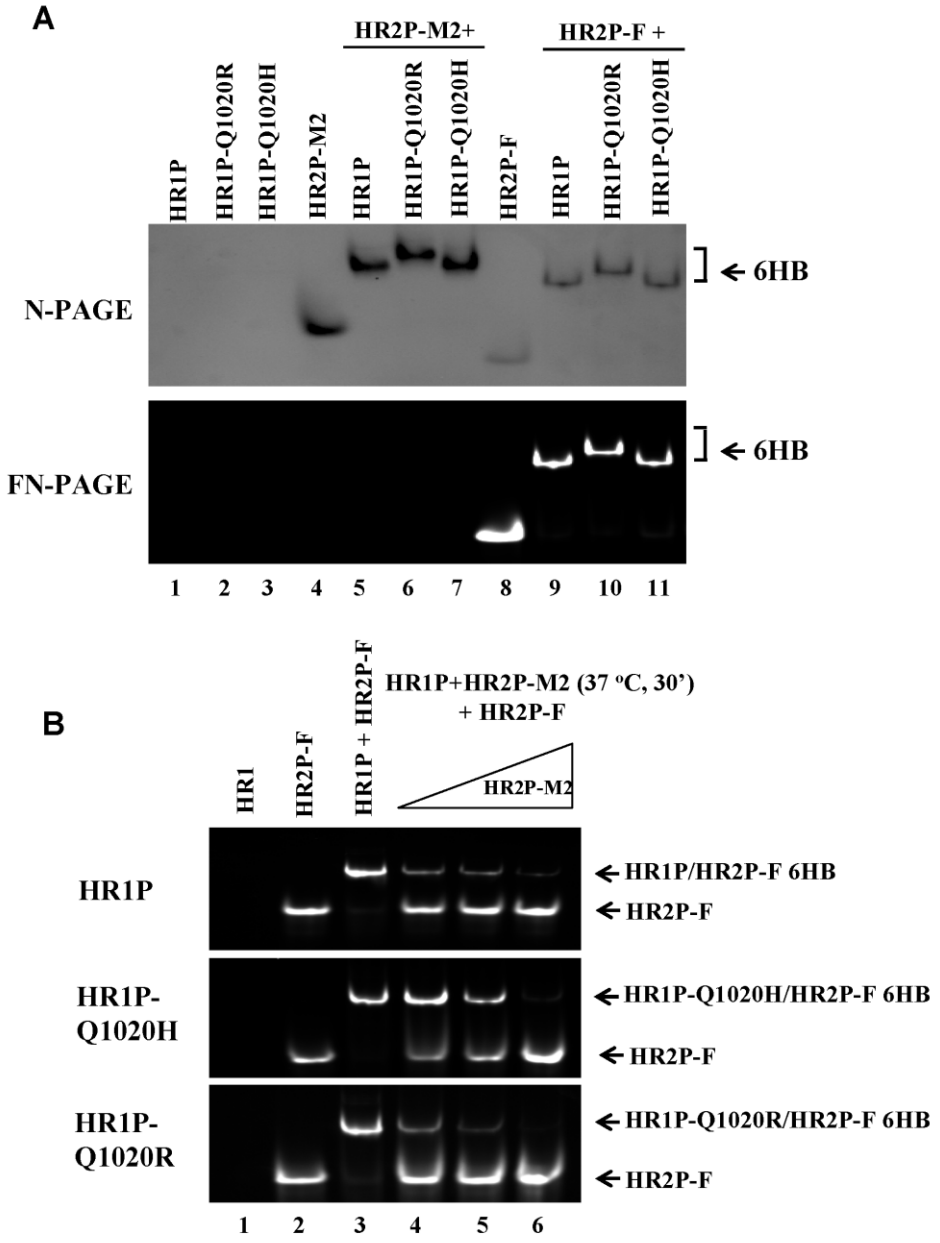

Figure 3

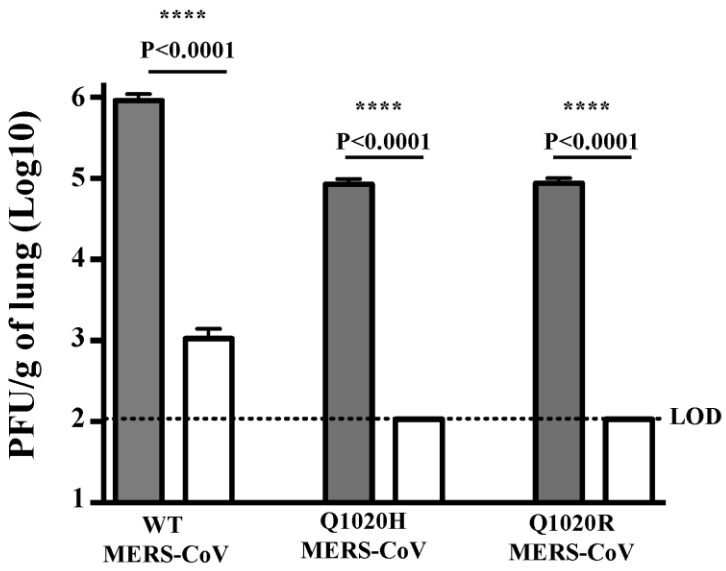

Figure 4

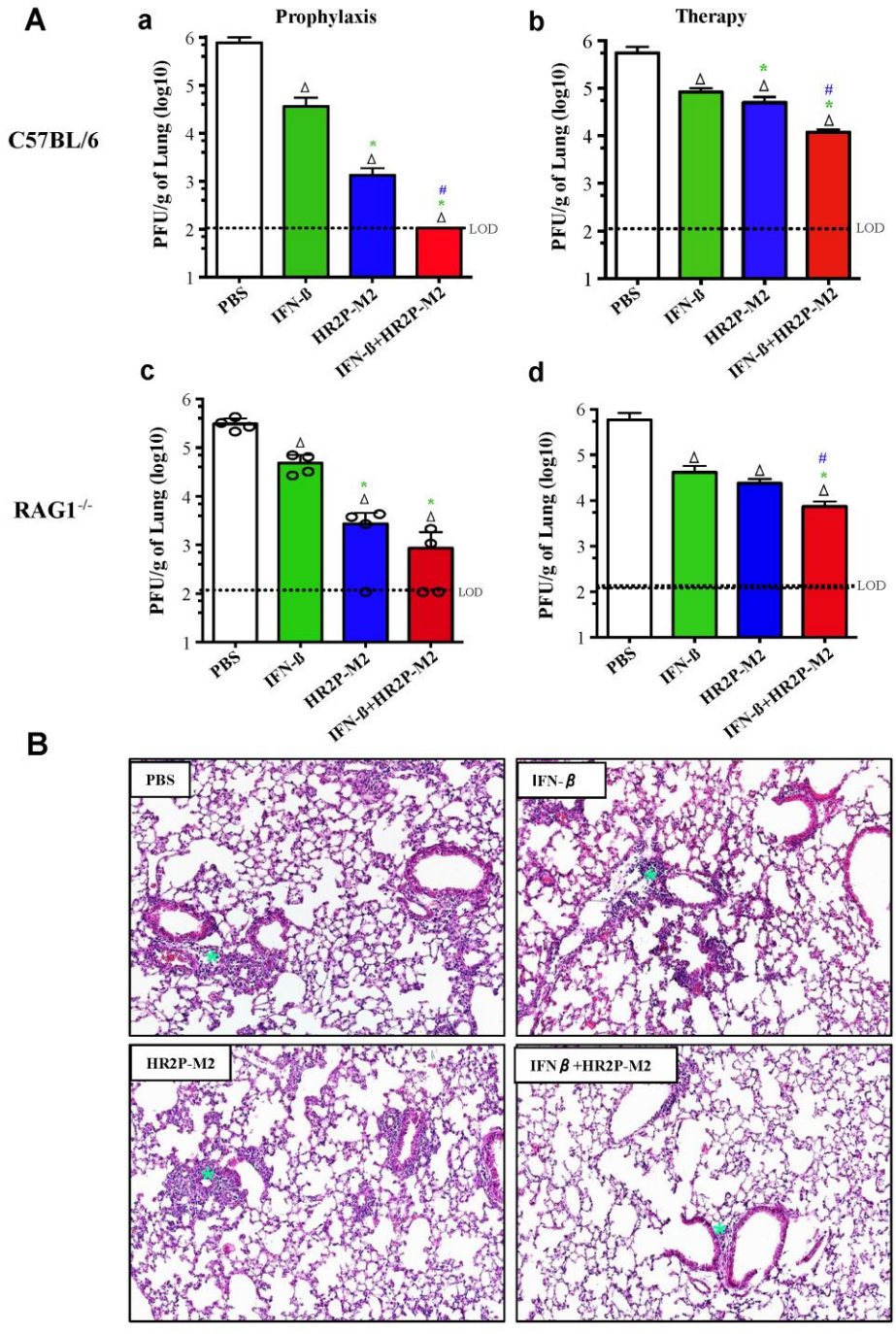

Figure 5